analytical chemistry

Article

pubs.acs.org/ac

High-Throughput Analysis of Ligand-Induced Internalization of β_2-Adrenoceptors Using the Coiled-Coil Tag−Probe Method

Yuki Takeda, Yoshiaki Yano, and Katsumi Matsuzaki*

Graduate School of Pharmaceutical Sciences, Kyoto University, Sakyo-ku, Kyoto 606-8501, Japan

Supporting Information

ABSTRACT: Receptor internalization is a useful indicator of the activity of ligands. The N-terminus of the β_2-adrenergic receptor expressed on the cell surface was labeled with fluorophores using a novel coiled-coil labeling system. Endocytosis of the receptors was automatically detected using a fluorescence image analyzer by evaluating (1) translocation of the receptor from cell-surface to intracellular regions and (2) acidification in endosomes. Both parameters increased upon agonist stimulation in a dose-dependent manner. The extent of endocytosis was significantly dependent on the agonist used, indicating the presence of a biased signaling for endocytosis. The receptor antagonists can also be screened by competitive inhibition of agonist-induced endocytosis. The image analysis approach has proven to be useful for high-throughput characterization and screening of GPCR ligands.

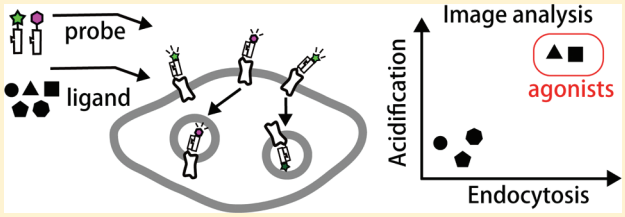

G-protein-coupled receptors (GPCRs) are one of the most important protein families for drug targets. The activation of GPCRs evokes complex responses in cells. For example, the β_2-adrenergic receptor (β2AR), which classically couples to Gα_s, can also activate Gα_i and mitogen-activated kinase signaling pathways.[1] Furthermore, β2AR and a majority of other GPCRs are desensitized and internalized into endosomes upon stimulation with agonists.[2,3] The ability of an agonist to activate these multiple pathways is often biased (conceptualized as "ligand-directed signaling"),[1,4] implying that GPCRs have multiple active conformations that can be stabilized by distinct ligands. Because of this complexity, a variety of cell-based detection methods are needed to find and characterize ligands for GPCRs.

Receptor desensitization/internalization is a promising indicator of the activation of GPCRs including orphan receptors because it is a ubiquitous process independent of downstream pathways.[1,5] Usually, the receptors *per se*[6−8] or β-arrestins[9] that bind to them upon internalization are fused with fluorescent proteins, and the receptor desensitization is detected by fluorescence imaging. However, the use of fluorescence proteins has several limitations.[10,11] The large size of fluorescent proteins (e.g., ∼27 kDa for GFP) can disrupt the normal trafficking and function of target proteins. Furthermore, fluorescent proteins inevitably label receptors even in intracellular compartments, which can obscure observations of internalization.

Recently, tag−probe labeling methods using genetically tagged proteins and exogenous probes that specifically bind to the tag have been shown to be advantageous over conventional assays with fluorescent proteins.[11,12] We have developed the coiled-coil tag−probe method based on a peptide pair (E3 tag $(EIAALKE)_3$ and K4 probe $(KIAALEK)_4$) that forms a heterodimeric coiled-coil structure.[13] The tag−probe pair (5−6 kDa) is much smaller than fluorescent proteins. Quick (within 1 min) and cell-surface specific labeling is particularly advantageous when observing the internalization of cell-surface receptors. Taking advantage of the ease of multicolor labeling, we have recently established a simple and sensitive method for the detection of receptor internalization based on fluorescence ratiometric imaging of the pH in endosomes.[10] Confocal microscopic observation of β2ARs doubly labeled with pH-dependent fluorescein (FL) and pH-independent tetramethylrhodamine (TMR) demonstrated a significant decrease in pH in endosomes after incubation with agonists in a concentration-dependent manner.

In this study, we performed automated image analysis using the high content screening reader ArrayScan (Thermo Scientific, Pittsburgh, PA) based on this approach to develop a novel cell-based method useful for ligand screening. Small-scale screening experiments revealed that the analysis method is useful for characterization of both receptor agonists and antagonists.

EXPERIMENTAL SECTION

Peptide Synthesis. The K4 peptide $(KIAALKE)_4$ was synthesized by a standard Fmoc-based solid phase method.[13] Fluorophores (TMR or FL) were labeled at the N-terminus by treatment with 5- (and 6)-carboxytetramethylrhodamine, succinimidyl ester or 5- (and 6)-carboxyfluorescein, succinimidyl ester, respectively.[13] The purity of the synthesized peptides (higher than 95%) was determined by analytical HPLC and ion spray mass spectrometry.

Received: December 6, 2011
Accepted: January 13, 2012
Published: January 13, 2012

   dx.doi.org/10.1021/ac203231n | *Anal. Chem.* 2012, 84, 1754−1759

Table 1. Index Values of Acidification and Endocytosis (n = 3) for 94 Compounds in Agonist and Antagonist Assays

	agonist assay		antagonist assay		
compd	% relative acidification	% relative endocytosis	% relative acidification	% relative endocytosis	description
			Agonists		
isoproterenol	100	100	100	100	β-adrenoceptor agonist
epinephrine	122 ± 31	102 ± 20	119 ± 14	106 ± 6	adrenoceptor agonist
norepinephrine	74 ± 9	66 ± 9	122 ± 5	117 ± 15	adrenoceptor agonist
procaterol	116 ± 32	84 ± 11	133 ± 10	130 ± 7	β2-adrenoceptor agonist
fenoterol	114 ± 16	88 ± 1	117 ± 34	112 ± 10	β2-adrenoceptor agonist
salbutamol	63 ± 43	46 ± 16	111 ± 10	122 ± 7	β2-adrenoceptor agonist
terbutaline	53 ± 16	60 ± 19	107 ± 18	115 ± 22	β2-adrenoceptor agonist
tulobuterol	2 ± 8	−24 ± 21	68 ± 29	70 ± 23	β2-adrenoceptor agonist
mabuterol	16 ± 11	−5 ± 13	49 ± 21	33 ± 4	β2-adrenoceptor agonist
clenbuterol	19 ± 18	18 ± 11	60 ± 25	52 ± 14	β2-adrenoceptor agonist
salmeterol	4 ± 17	16 ± 16	40 ± 8	32 ± 1	β2-adrenoceptor agonist
ritodrine	20 ± 3	−5 ± 14	84 ± 11	103 ± 28	β2-adrenoceptor agonist
			Antagonists		
propranolol[a]	47 ± 24	42 ± 16	10 ± 18	4 ± 7	β-adrenoceptor antagonist
pindolol	22 ± 18	0 ± 7	3 ± 3	−12 ± 6	β-adrenoceptor antagonist
alprenolol	−1 ± 7	−3 ± 12	19 ± 8	−3 ± 6	β-adrenoceptor antagonist
timolol[a]	139 ± 29	218 ± 27	34 ± 7	18 ± 13	β-adrenoceptor antagonist
labetalol	31 ± 9	9 ± 5	18 ± 24	3 ± 20	α-and β-adrenoceptor antagonist
amosulalol	24 ± 20	5 ± 12	49 ± 19	17 ± 14	α-and β-adrenoceptor antagonist
			Other Drugs		
phenilephrine	14 ± 8	3 ± 10	113 ± 16	136 ± 15	α1-adrenoceptor agonist
naphazoline	34 ± 12	6 ± 1	109 ± 15	115 ± 16	α -adrenoceptor agonist
dobutamine	6 ± 7	−13 ± 10	84 ± 14	96 ± 9	β1 -adrenoceptor agonist
tyramine	23 ± 7	7 ± 15	97 ± 11	111 ± 11	catecholamine releasing agent
dopamine	29 ± 12	14 ± 4	104 ± 18	131 ± 12	dopamine receptor agonist
prazosin	24 ± 15	9 ± 12	105 ± 16	148 ± 20	α1-adrenoceptor antagonist
acebutolol	17 ± 18	11 ± 8	96 ± 20	96 ± 11	β1-adrenoceptor antagonist
L-atenolol[a]	75 ± 13	96 ± 21	105 ± 15	87 ± 15	β1-adrenoceptor antagonist
D-atenolol	36 ± 18	11 ± 8	154 ± 8	129 ± 15	β1-adrenoceptor antagonist
clonidine	18 ± 13	9 ± 5	111 ± 25	111 ± 17	α2-adrenoceptor agonist
acetylcholine	33 ± 3	9 ± 7	114 ± 19	116 ± 12	cholinoceptor agonist
atropine	25 ± 13	14 ± 13	124 ± 9	115 ± 7	muscarinic acetylcholine receptor antagonist
procaine	23 ± 20	9 ± 12	115 ± 19	98 ± 6	local anesthetic
tubocurarine	30 ± 20	8 ± 6	139 ± 18	118 ± 12	nondepolarizing neuromuscular blocker
suxamethonium	6 ± 5	−1 ± 10	104 ± 6	103 ± 20	depolarizing neuromuscular blocker
baclofen	31 ± 18	15 ± 4	124 ± 9	123 ± 14	skeletal muscle relaxant; $GABA_B$ receptor agonist
chlorpromazine[a]	34 ± 13	59 ± 29	92 ± 16	103 ± 36	dopamine receptor antagonist
haloperidol	21 ± 15	6 ± 7	96 ± 7	104 ± 7	dopamine receptor antagonist
sulpiride	36 ± 29	9 ± 12	113 ± 8	115 ± 15	dopamine receptor antagonist
lithium carbonate	14 ± 14	−2 ± 14	102 ± 13	108 ± 6	prophylaxis of affective disorders
imipramine[a]	54 ± 13	31 ± 5	87 ± 13	109 ± 6	monoamine reuptake inhibitor; α1-adrenoceptor antagonist
desipramine[a]	68 ± 7	114 ± 16	76 ± 9	85 ± 6	monoamine reuptake inhibitor; α1-adrenoceptor antagonist
mianserin	26 ± 14	4 ± 13	101 ± 15	95 ± 6	monoamine reuptake inhibitor
fluvoxamine	9 ± 1	−5 ± 5	103 ± 5	105 ± 3	selective serotonin reuptake inhibitor
phenytoin	16 ± 17	9 ± 9	110 ± 7	108 ± 8	antiepileptic
antipyrine	3 ± 24	13 ± 14	105 ± 16	118 ± 12	pyrazolone class analgesic agent
cyclosporin A	4 ± 2	35 ± 5	101 ± 25	133 ± 4	immunosuppressant drug
cyclophosphamide	10 ± 7	0 ± 11	105 ± 27	125 ± 30	cytotoxic alkylating agent
methotrexate	12 ± 3	−1 ± 4	103 ± 7	114 ± 4	dihydrofolate reductase inhibitor
zidovudine	22 ± 14	8 ± 2	109 ± 12	111 ± 1	nucleoside reverse transcriptase inhibitor
diphenhydramine	−10 ± 18	3 ± 24	103 ± 15	113 ± 21	histamine H1 receptor antagonist
cimetidine	24 ± 14	3 ± 14	103 ± 16	108 ± 13	histamine H2 receptor antagonist
granisetron	8 ± 6	−8 ± 5	101 ± 13	109 ± 11	serotonin 5HT3 receptor antagonist
sumatriptan	11 ± 11	−5 ± 10	96 ± 23	97 ± 15	serotonin 5HT1 receptor agonist
captopril	−3 ± 8	−5 ± 4	106 ± 28	107 ± 10	angiotensin converting enzyme inhibitor
ozagrel	20 ± 6	−l ± 11	88 ± 13	106 ± 24	thromboxane A2 synthesis inhibitor
aspirin	14 ± 16	−6 ± 12	91 ± 7	103 ± 1	salicylate; nonselective cyclo-oxygenase inhibitor
indometacin	−1 ± 9	3 ± 4	95 ± 14	109 ± 16	cyclo-oxygenase inhibitor

dx.doi.org/10.1021/ac203231n | Anal. Chem. 2012, 84, 1754−1759

Table 1. continued

compd	agonist assay		antagonist assay		description
	% relative acidification	% relative endocytosis	% relative acidification	% relative endocytosis	
			Other Drugs		
phenylbutazone	−3 ± 19	−6 ± 12	95 ± 16	109 ± 12	cyclo-oxygenase inhibitor
penicillamine	33 ± 8	5 ± 19	100 ± 18	98 ± 18	antirheumatic drug; chelating agent
digitoxin	7 ± 19	1 ± 6	95 ± 31	103 ± 18	Na/K-ATPase inhibitor
digoxin	8 ± 16	0 ± 9	94 ± 2	107 ± 12	Na/K-ATPase inhibitor
quinidine	10 ± 2	5 ± 5	82 ± 3	97 ± 8	class I antiarrhythmic
lidocaine	20 ± 7	9 ± 4	157 ± 12	121 ± 6	local anesthetic; class I antiarrhythmic; sodium channel blocker
amiodarone	31 ± 24	−5 ± 8	143 ± 11	128 ± 14	potassium channel blocker
nifedipine	4 ± 8	−12 ± 4	139 ± 30	126 ± 8	calcium channel blocker
flunarizine	−10 ± 23	11 ± 9	162 ± 57	147 ± 27	calcium channel blocker
dextromethorphan	15 ± 10	2 ± 19	123 ± 38	124 ± 33	opioid receptor agonist
guaifenesin	29 ± 20	1 ± 13	123 ± 10	118 ± 7	expectorant
sodium cromoglicate	23 ± 10	2 ± 3	99 ± 27	103 ± 16	prophylaxis of allergic conditions; prevents the release of inflammatory chemicals
theophylline	25 ± 16	1 ± 2	161 ± 8	128 ± 4	nonselective phosphodiesterase inhibitor (xanthine)
prednisolone	−4 ± 16	0 ± 1	119 ± 10	113 ± 21	glucocorticoid
acetazolamide	10 ± 12	−2 ± 11	121 ± 12	107 ± 19	carbonic anhydrase inhibitor
hydrochlorothiazide	17 ± 10	−3 ± 6	123 ± 34	117 ± 18	thiazide diuretic
furosemide	19 ± 12	7 ± 12	148 ± 48	135 ± 5	loop diuretic
spironolactone	12 ± 27	−6 ± 18	150 ± 20	129 ± 2	aldosterone receptor antagonist
triamterene	−13 ± 3	−2 ± 1	131 ± 18	176 ± 21	sodium channel blocker
papaverine[a]	76 ± 8	37 ± 12	264 ± 23	274 ± 16	phosphodiesterase inhibitor; α2-adrenoceptor antagonist
heparin sodium	−112 ± 2	−23 ± 7	−123 ± 2	11 ± 11	anticoagulant
tranexamic acid	23 ± 14	5 ± 7	78 ± 3	108 ± 22	antifibrinolytic
tolbutamide	21 ± 10	10 ± 6	131 ± 35	107 ± 16	inhibition of ATP-dependent potassium channels
glibenclamide	10 ± 17	3 ± 4	147 ± 28	143 ± 28	inhibition of ATP-dependent potassium channels
buformin	2 ± 13	4 ± 22	83 ± 24	93 ± 12	antidiabetic drug of the biguanide class
acarbose	9 ± 7	0 ± 3	101 ± 11	106 ± 8	α-glucosidase inhibitor
simvastatin	−19 ± 16	54 ± 12	113 ± 24	181 ± 34	HMG Co-A reductase inhibitor
probucol	17 ± 12	2 ± 4	108 ± 12	117 ± 11	antihyperlipidemic drug; lowers the level of cholesterol in the bloodstream
colchicine[a]	47 ± 26	61 ± 17	62 ± 44	66 ± 26	used in treatment of gout; inhibits microtubule polymerization by binding to tubulin
allopurinol	20 ± 25	5 ± 4	131 ± 10	132 ± 24	xanthine oxidase inhibitor
etidronic acid	10 ± 17	−11 ± 13	84 ± 14	111 ± 10	bisphosphonate; chelating agent
rifampicin	23 ± 13	11 ± 10	89 ± 10	123 ± 6	rifamycin antituberculosis drug; DNA-dependent RNA polymerase inhibitor
itraconazole	13 ± 10	−3 ± 4	87 ± 11	96 ± 5	triazole antifungal agent antifungal
vidarabine	16 ± 6	6 ± 9	95 ± 31	105 ± 37	antiviral drug; inhibts the synthesis of viral
mercaptopurine	15 ± 9	−2 ± 7	118 ± 19	107 ± 3	thiopurine cytotoxic; inhibits purine nucleotide synthesis and metabolism
5-fluorourcial	11 ± 18	−6 ± 8	109 ± 21	112 ± 12	pyrimidine analogue; inhibits of thymidylate synthase
doxifluridine	19 ± 17	−1 ± 7	112 ± 23	122 ± 12	pyrimidine analogue; inhibits of thymidylate synthase
tamoxifen[a]	15 ± 18	88 ± 13	125 ± 44	149 ± 60	selective estrogen receptor modulator

[a]The compounds that exhibited false-positive signals in the agonist assay.

Cell Culture. Flp-In Chinese hamster ovary (CHO) cells stably expressing E3-tagged β_2-adrenergic receptors (E3-β2ARs)[10] were cultured in F-12 medium with 10% heat-inactivated fetal bovine serum (FBS) and hygromycin (500 μg/mL) in a humidified incubator at 37 °C, 5% CO_2. For measurements using an ArrayScan VTI HCS reader, cells were seeded (13 000 cells/well) into black 96-well glass bottom plates (Thermo Scientific) and cultured in F-12 supplemented with 10% FBS and penicillin/streptomycin for 48 h at 37 °C, 5% CO_2.

Measurement of Receptor Internalization. TMR-K4 and FL-K4 probes were mixed in 0.01 N NaOH to give a stock solution (10 μM each) and diluted in PBS (+) to obtain a labeling solution (20 nM each). Cells were incubated with 100 μL of the labeling solution for 2 min.

For time-dependence measurements, 20 μM isoproterenol (Iso) dissolved in 100 μL of PBS (+) containing 0.02% DMSO was added to a well filled with 100 μL of the labeling solution to give a final concentration of 10 μM (0.01% DMSO). Control experiments were similarly performed without Iso. At the same time, the cells were stained with Hoechst 33342 (2 μg/mL). After incubation for 30 min at 37 °C, the plate was transferred to an ArrayScan apparatus, and fluorescence images were acquired at intervals of 15 min at room temperature. In fixation experiments, the cells were fixed with neutral buffered 4% formalin for 30 min at room temperature after the incubation with Iso. To obtain the dose−response curves of receptor

dx.doi.org/10.1021/ac203231n | Anal. Chem. 2012, 84, 1754−1759

internalization for ligands, cells were treated with increasing concentrations of agonist or antagonist (containing 1 μM Iso). EC_{50} and IC_{50} values were determined by fitting the data with the following equations: Top + (Bottom − Top)/(1 + $10^{[L]-\log(EC50)}$), and Bottom + (Top − Bottom)/(1 + $10^{[L]-\log(IC50)}$), respectively, where [L] denotes the concentration of the ligands on a log scale. For the agonist assay, each of 94 compounds including 12 agonists and 6 antagonists (Table 1) was added at a final concentration of 10 μM. For the antagonist assay, each of 94 compounds was added at a final concentration of 10 μM in the presence of 1 μM Iso.

Image Acquisition and Analysis Using ArrayScan. The automated acquisition of fluorescence images and analysis were performed on a ArrayScan VTI HCS reader. Four regions per well were imaged using a 20× objective lens. Hoechst 33342 (Ex 386 nm; Em 505−525 nm), FL (Ex 480 nm; Em 505−525 nm), and TMR (Ex 549 nm; Em 570−610 nm) images were sequentially acquired to avoid crosstalk of the fluorescence. Hoechst 33342 fluorescence was used to automatically focus on the nucleus. The "compartmental analysis" software was used to quantify receptor internalization. The objects used for the analysis of internalization were selected on the basis of fluorescence images of Hoechst 33342 (average intensity 0−1500; pixel area 100−400; objectshapeP2A 0.1−2.1; objectshapeLWR 0.1−1.8). The intracellular region and plasma membrane region were defined on the basis of the nuclear region. The intracellular region, designated as a "circle", was defined as an area 5 pixels larger than the nuclear region. The plasma membrane region or "ring" was defined as a doughnut-shaped area that has a 5-pixel width from the intracellular "circle" (see Figure 1B). Indices for acidification ($F^{TMR}_{circle}/F^{FL}_{circle}$) and endocytosis ($F^{TMR}_{circle}/F^{TMR}_{ring}$) were used to evaluate the extent of the receptor internalization. The values were normalized by defining DMSO and Iso controls as 0% and 100%, respectively.

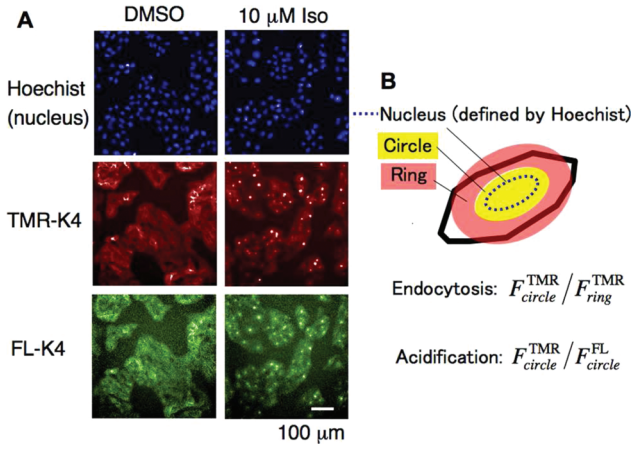

Figure 1. Evaluation of receptor endocytosis by image analyzer (ArrayScan). (A) Examples of fluorescence images in the absence and presence of agonist. E3-β2ARs stably expressed on CHO cells were stained with three fluorophores (Hoechst 33342 for labeling of the nucleus and TMR-K4 and FL-K4 for labeling of the receptor). (B) Schematic illustration of parameters used to evaluate the endocytosis of the receptor. The circle and ring regions were automatically determined from the region of the nucleus (see Experimental Section in detail).

Calculation of *Z′* Factor. To calculate the Z' factor, one-half of a 96-well plate was treated with 10 μM Iso-containing 0.01% DMSO (positive control), while the other half was treated with 0.01% DMSO (negative control) for 30 min at 37 °C, and images were acquired after 15 min incubation at room temperature. The measurement was repeated on three consecutive days. Z' values were calculated using the following formula: $Z' = 1 - (3\sigma_p + 3\sigma_n)/|\mu_p - \mu_n|$.[14] The symbols μ and σ indicate the average and standard deviation, respectively. Subscripts p and n mean the values for positive and negative controls, respectively.

RESULTS AND DISCUSSION

For detection of the decrease in pH in endosomes, E3-β2ARs stably expressed on CHO cells were doubly labeled with TMR-K4 and FL-K4 probes as reported previously.[10] Furthermore, a nuclear staining reagent (Hoechst 33342) was used to automatically determine the position of the nucleus. Examples of the fluorescence images obtained with the image analyzer (ArrayScan) in the absence and presence of the agonist Iso are shown in Figure 1A. Two parameters were used to evaluate receptor internalization (Figure 1B). One parameter is a measure of endocytosis ($F^{TMR}_{circle}/F^{TMR}_{ring}$) which evaluates the translocation of receptors from the cell surface to intracellular regions; the other represents the extent of acidification ($F^{TMR}_{circle}/F^{FL}_{circle}$), which quantifies pH changes in endosomes. The F^{FL}_{circle} value decreases at acidic pH, whereas the F^{TMR}_{circle} value is pH-independent. Both indices increase with the progression of endocytosis.

To stabilize samples for a prolonged period, we first examined the effect of cell fixation. However, the addition of formalin significantly decreased the intensity of both TMR and FL (data not shown), and the measures of endocytosis and acidification changed significantly during the measurement period (Figure S1C,D in the Supporting Information). Therefore, we examined the stability of the receptor internalization in living cells. Treatment with 10 μM Iso increased the indices of acidification and endocytosis by ∼2 and ∼1.5 times, respectively (Figure S1A,B in the Supporting Information). Both values remained virtually constant from 15 to 60 min at room temperature after incubation with Iso for 30 min at 37 °C. Therefore, we started the ArrayScan measurements 15 min after the incubation at room temperature without fixation in subsequent experiments. The acquisition time for 96-well plates (∼8 min) is sufficiently short to obtain stable signals. For endocytosis and acidification, the Z' factor values were 0.30 ± 0.08 and −1.0 ± 0.8, respectively (n = 3).

We next examined the dose dependence of the extent of receptor internalization using the full agonist Iso and the partial agonist salbutamol. The acidification and endocytosis values increased with similar dose-dependences (Figure 2A,B). The EC_{50} values for Iso-dependent receptor internalization were 37 ± 7 nM (acidification) and 26 ± 11 nM (endocytosis), which agreed well with previously reported values.[6] The acidification EC_{50} value was smaller than that previously obtained from confocal images (176 ± 76 nM),[10] probably because the present image analysis focuses on the intracellular region whereas the confocal study analyzed signals from whole cells. EC_{50} values for receptor internalization induced by salbutamol were 322 ± 155 nM (acidification) and 256 ± 163 nM (endocytosis).

We also examined the inhibitory effects of the antagonist propranolol on the Iso-induced internalization of receptors. Acidification and endocytosis values decreased with similar dose-dependence (Figure 2C,D) (IC_{50}: 1.7 ± 0.6 nM for

dx.doi.org/10.1021/ac203231n | Anal. Chem. 2012, 84, 1754−1759

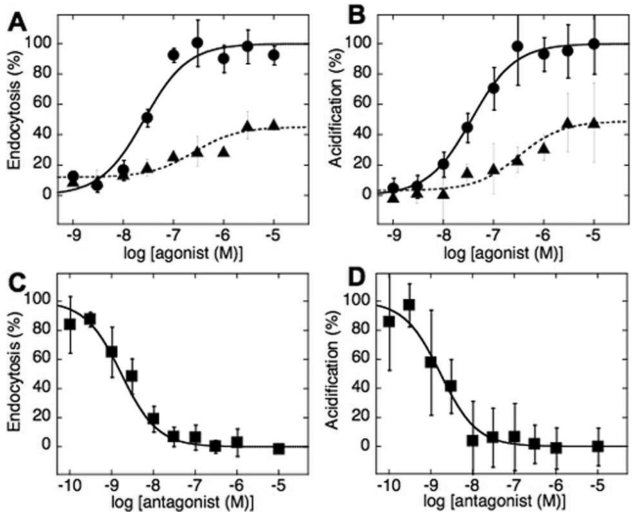

Figure 2. Dose−response curves for agonists (A, B) and antagonists (C, D). The maximal response for Iso was defined as 100%. (A, B) The extent of endocytosis estimated from endocytosis (A) and acidification (B) for Iso (circles) and salbutamol (triangles). The data were fitted with sigmoidal curves as described in the Experimental Section. (C, D) Competitive inhibition of Iso-induced endocytosis with the antagonist propranolol evaluated by endocytosis (C) and acidification (D). The concentration of Iso was fixed at 1 μM.

acidification and 2.2 ± 0.5 nM for endocytosis). The above results clearly show that the efficacy of receptor agonists and antagonists can be evaluated by the image analysis of endocytosis of the receptors.

We further examined the extent of acidification and endocytosis using 94 compounds including 12 agonists and 6 antagonists (Table 1) at a fixed concentration of 10 μM. For the agonist assay, both the acidification and endocytosis values increased in cells incubated with six agonists (Figure 3A and Table 1). Three of the six agonists (epinephrine, procaterol, and fenoterol) showed similar efficacy to Iso, and the other three (norepinephrine, salbutamol, and terbutaline) exhibited about 50% of the maximum response. Conversely, five agonists (tulobuterol, mabuterol, clenbuterol, salmeterol, and ritodrine) did not promote receptor internalization. The observed endocytotic properties of the agonists did not correlate with the binding affinity, EC_{50} values determined from cAMP production, or maximal cAMP response (see Table 4 in ref 15), although agonists that did not promote endocytosis tended to have lower efficacy ratios (intrinsic efficacies).[15] Note that the ligand concentration used here (10 μM) is sufficiently higher than the dissociation constants except in the case of ritodrine. These results strongly suggest the presence of ligand-directed signaling for an endocytotic pathway independent of the cAMP signaling pathway. Interestingly, most of the observed non-endocytotic agonists (except ritodrine) are known as long-acting β_2 agonists,[16−19] consistent with longer stimulation of the receptor without desensitization.[20,21]

The agonist assay identified nine false-positive compounds that apparently increased the extent of acidification and endocytosis (marked with asterisks in Table 1 and Figure 3A). However, they did not induce any redistribution of receptors from the plasma membrane to intracellular region, as confirmed by confocal microscopy (Figure S2 in the Supporting Information). Rather, rounding of cells was often observed after treatment with the false-positive compounds. Translocation of the cell membrane from the ring to circle area due to rounding can result in an apparent increase in endocytosis. We also found that most of the false-positive compounds were antagonists for adrenaline or dopamine receptors, except colchicine and tamoxifen.[22−26] These antagonists may bind to E3-β2ARs and increase the values for endocytosis and acidification. Another possibility is indirect induction of the internalization by distinct pathways, as reported for insulin.[27]

For the antagonist assay, Iso-induced acidification and endocytosis were inhibited by coincubation with antagonists of the receptor (Figure 3B). All the antagonists significantly suppressed both acidification and endocytosis to the level of the negative control. Furthermore, most of the agonists that did not induce receptor internalization inhibited Iso-induced receptor internalization by competitively inhibiting the binding of Iso (triangles in Figure 3B), although ritodrine could not inhibit the internalization because of insufficient affinity.[15] Therefore,

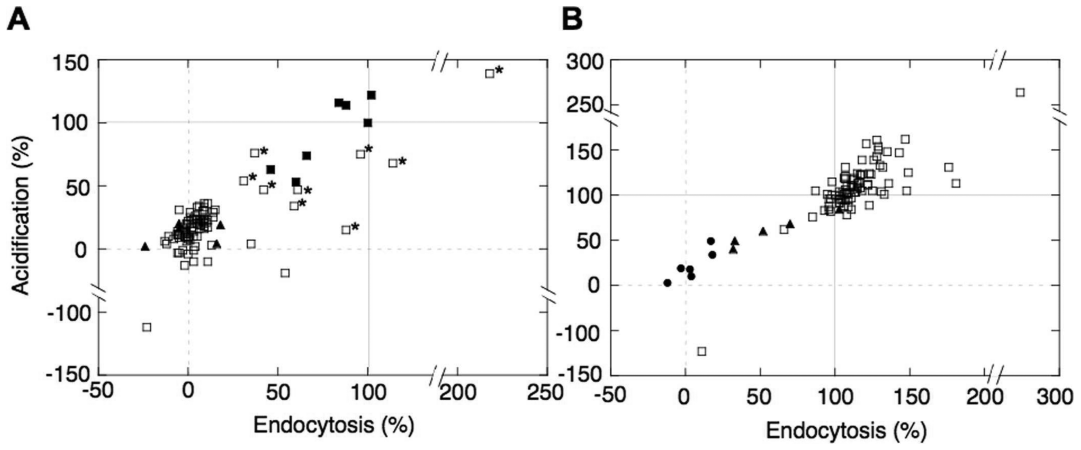

Figure 3. Small-scale screening of agonists (A) and antagonists (B). The concentration of the screened compounds was fixed at 10 μM. In the antagonist assay, the concentration of isoproterenol was fixed at 1 μM. The plots show values for endocytosis (*X*-axis) and acidification (*Y*-axis). The agonists that promoted receptor internalization, the agonists that did not promote receptor internalization, and the antagonists are represented by solid squares, solid triangles, and solid circles, respectively. Other compounds are represented by open squares. The compounds that exhibited false-positive signals in the agonist screening are marked with asterisks.

dx.doi.org/10.1021/ac203231n | *Anal. Chem.* 2012, 84, 1754−1759

agonists that do not cause receptor internalization can be detected in the antagonist assay.

We assessed the accuracy of the agonist and antagonist assays by using receiver operating characteristic (ROC) curves.[28] The curves were obtained by calculating the sensitivity and specificity of an assay at every possible cutoff point, and plotting sensitivity against (1 − specificity).[28] The area under the curve (AUC) is an indicator for the accuracy of the test. A greater AUC means a better assay (a perfect assay will have an AUC of unity). In the antagonist assay, we calculated ROC curves in two cases: (1) only antagonists were classified as positive and (2) agonists that did not promote receptor internalization were also counted as positive. Both agonist and antagonist assays had AUC values larger than 0.95 for acidification and endocytosis (Figure 4), indicating that these assays are useful for ligand screening.

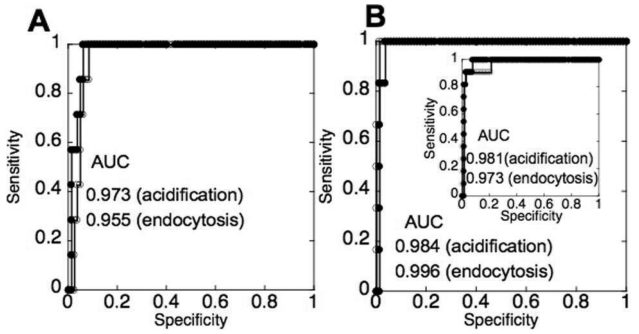

Figure 4. Receiver operating characteristic (ROC) curves for the agonist assay (A) and antagonist assay (B). Open circles and closed circles indicate the curves for endocytosis and acidification, respectively. The AUC values are shown in the graph. The antagonist assay was tested assuming that only antagonists are true positives. The inset shows the analysis assuming that both antagonists and agonists that do not promote endocytosis are true positives.

CONCLUSIONS

We demonstrated by image acquisition and ArrayScan that two complementary approaches, acidification and endocytosis, could be used to quantify the agonist-induced internalization of β2ARs and antagonist-induced inhibition of the internalization. This approach has proven useful for the characterization of GPCR ligands in terms of receptor endocytosis. It will also be a valuable tool for high-throughput ligand screening, particularly to find antagonists that inhibit receptor internalization.

ASSOCIATED CONTENT

Supporting Information

Stability of the endocytosis signals and confocal images after incubation with false-positive compounds. This material is available free of charge via the Internet at http://pubs.acs.org.

AUTHOR INFORMATION

Corresponding Author

*Phone: 81-75-753-4521. Fax: 81-75-753-4578. E-mail: mkatsumi@pharm.kyoto-u.ac.jp.

ACKNOWLEDGMENTS

This work was financially supported in part by the Targeted Proteins Research Program of MEXT, Japan. We thank Drs. Shinya Oishi and Nobutaka Fujii (Kyoto University) for technical advice on peptide synthesis.

REFERENCES

(1) Evans, B. A.; Sato, M.; Sarwar, M.; Hutchinson, D. S.; Summers, R. J. *Br. J. Pharmacol.* **2010**, *159*, 1022−1038.
(2) Wolfe, B. L.; Trejo, J. *Traffic* **2007**, *8*, 462−470.
(3) Mukherjee, S.; Ghosh, R. N.; Maxfield, F. R. *Physiol. Rev.* **1997**, *77*, 759−803.
(4) Michel, M. C.; Alewijnse, A. E. *Mol. Pharmacol.* **2007**, *72*, 1097−1099.
(5) Zhao, X.; Jones, A.; Olson, K. R.; Peng, K.; Wehrman, T.; Park, A.; Mallari, R.; Nebalasca, D.; Young, S. W.; Xiao, S. H. *J. Biomol. Screening* **2008**, *13*, 737−747.
(6) Fukunaga, S.; Setoguchi, S.; Hirasawa, A.; Tsujimoto, G. *Life Sci.* **2006**, *80*, 17−23.
(7) Kallal, L.; Benovic, J. L. *Trends Pharmacol. Sci.* **2000**, *21*, 175−180.
(8) Conway, B. R.; Minor, L. K.; Xu, J. Z.; Gunnet, J. W.; DeBiasio, R.; D'Andrea, M. R.; Rubin, R.; Giuliano, K.; DeBiasio, L.; Demarest, K. T. *J. Biomol. Screening* **1999**, *4*, 75−86.
(9) Ross, D. A.; Lee, S.; Reiser, V.; Xue, J.; Alves, K.; Vaidya, S.; Kreamer, A.; Mull, R.; Hudak, E.; Hare, T.; Detmers, P. A.; Lingham, R.; Ferrer, M.; Strulovici, B.; Santini, F. *J. Biomol. Screening* **2008**, *13*, 449−455.
(10) Yano, Y.; Matsuzaki, K. *FEBS Lett.* **2011**, *585*, 2385−2388.
(11) Yano, Y.; Matsuzaki, K. *Biochim. Biophys. Acta* **2009**, *1788*, 2124−2131.
(12) Ward, R. J.; Pediani, J. D.; Milligan, G. *Br. J. Pharmacol.* **2011**, *162*, 1439−1452.
(13) Yano, Y.; Yano, A.; Oishi, S.; Sugimoto, Y.; Tsujimoto, G.; Fujii, N.; Matsuzaki, K. *ACS Chem. Biol.* **2008**, *3*, 341−345.
(14) Zhang, J. H.; Chung, T. D.; Oldenburg, K. R. *J. Biomol. Screening* **1999**, *4*, 67−73.
(15) Baker, J. G. *Br. J. Pharmacol.* **2010**, *160*, 1048−1061.
(16) Nials, A. T.; Coleman, R. A.; Johnson, M.; Magnussen, H.; Rabe, K. F.; Vardey, C. J. *Br. J. Pharmacol.* **1993**, *110*, 1112−1116.
(17) Johnson, M. *Lung* **1990**, *168* (Suppl), 115−119.
(18) Aldons, P. M. *Lung* **1990**, *168* (Suppl), 186−191.
(19) Murai, T.; Maejima, T.; Sanai, K.; Osada, E. *Arzneimittelforschung* **1984**, *34*, 1633−1640.
(20) Moore, R. H.; Millman, E. E.; Godines, V.; Hanania, N. A.; Tran, T. M.; Peng, H.; Dickey, B. F.; Knoll, B. J.; Clark, R. B. *Am. J. Respir. Cell Mol. Biol.* **2007**, *36*, 254−261.
(21) Kume, H. *Allergol. Int.* **2005**, *54*, 89−97.
(22) Baker, J. G. *Br. J. Pharmacol.* **2005**, *144*, 317−322.
(23) Papp, M.; Klimek, V.; Willner, P. *Psychopharmacology* **1994**, *114*, 309−314.
(24) Cusack, B.; Nelson, A.; Richelson, E. *Psychopharmacology* **1994**, *114*, 559−565.
(25) O'Hara, N.; Ono, H. *Life. Sci.* **1987**, *40*, 1301−1308.
(26) Fishman, P. H.; Finberg, J. P. *J. Neurochem.* **1987**, *49*, 282−289.
(27) Shumay, E.; Gavi, S.; Wang, H. Y.; Malbon, C. C. *J. Cell. Sci.* **2004**, *117*, 593−600.
(28) Vining, D. J.; Gladish, G. W. *Radiographics* **1992**, *12*, 1147−1154.